Hemin Therapy Improves Kidney Function in Male Streptozotocin-Induced Diabetic Rats: Role of the Heme Oxygenase/Atrial Natriuretic Peptide/Adiponectin Axis

Joseph Fomusi Ndisang and Ashok Jadhav

Department of Physiology, University of Saskatchewan College of Medicine, Saskatoon, Saskatchewan, Canada S7N 5E5

Diabetic nephropathy is characterized by elevated macrophage infiltration and inflammation. Although heme-oxygenase (HO) is cytoprotective, its role in macrophage infiltration and nephropathy in type 1 diabetes is not completely elucidated. Administering the HO inducer, hemin, to streptozotocin-diabetic rats suppressed renal proinflammatory macrophage-M1 phenotype alongside several proinflammatory agents, chemokines, and cytokines including macrophage inflammatory protein 1α (MIP-1α), macrophage-chemoattractant protein-1 (*MCP-1*), TNF-α, IL-1β, IL-6, nuclear factor-κB (NF-κB), and aldosterone, a stimulator of the inflammatory/oxidative transcription factor, NF-κB. Similarly, hemin therapy attenuated extracellular matrix/profibrotic proteins implicated in renal injury including fibronectin, collagen-IV, and TGF-β1 and reduced several renal histopathological lesions such as glomerulosclerosis, tubular necrosis, tubular vacuolization, and interstitial macrophage infiltration. Furthermore, hemin reduced markers of kidney dysfunction like proteinuria and albuminuria but increased creatinine clearance, suggesting improved kidney function. Correspondingly, hemin significantly enhanced the antiinflammatory macrophage-M2 phenotype, IL-10, adiponectin, HO-1, HO activity, and atrial natriuretic-peptide (ANP), a substance that abates TNF-α, IL-6, and IL-1β, with parallel increase of urinary cGMP, a surrogate marker of ANP. Contrarily, coadministering the HO inhibitor, chromium-mesoporphyrin with the HO-inducer, hemin nullified the antidiabetic and renoprotective effects, whereas administering chromium-mesoporphyrin alone abrogated basal HO activity, reduced basal adiponectin and ANP levels, aggravated hyperglycemia, and further increased MCP-1, MIP-1α, aldosterone, NF-κB, TNF-α, IL-6, IL-1β, proteinuria/albuminuria, and aggravated creatinine clearance, thus exacerbating renal dysfunction, suggesting the importance of the basal HO-adiponectin-ANP axis in renoprotection and kidney function. Collectively, these data suggest that hemin ameliorates diabetic nephropathy by selectively enhancing the antiinflammatory macrophage-M2 phenotype and IL-10 while concomitantly abating the proinflammatory macrophage-M1 phenotype and suppressing extracellular matrix/profibrotic factors with reduction of renal lesions including interstitial macrophage infiltration. Because aldosterone stimulate NF-κB, which activates cytokines like TNF-α, IL-6, IL-1β that in turn stimulate chemokines such as MCP-1 and MIP-1α to promote macrophage-M1 infiltration, the hemin-dependent potentiation of the HO-adiponectin-ANP axis may account for reduced macrophage infiltration and inflammatory insults in streptozotocin-diabetic rats. **(*Endocrinology* 155: 215–229, 2014)**

ISSN Print 0013-7227 ISSN Online 1945-7170
Printed in U.S.A.

Received January 11, 2013. Accepted October 7, 2013.
First Published Online October 18, 2013

Abbreviations: AMPK, AMP-activated protein kinase; ANP, atrial natriuretic-peptide; AP-1, activating-protein 1; BP, blood pressure; CrMP, chromium-mesoporphyrin; ED, activated macrophage; HO, heme-oxygenase; MCP-1, macrophage-chemoattractant protein-1; MIP-1α, macrophage inflammatory protein 1α; NF-κB, nuclear factor-κB; SD, Sprague Dawley; STZ, streptozotocin.

Diabetic nephropathy is a common microvascular complication in type 1 and type 2 diabetes mellitus. It is generally characterized by the progressive loss of renal function, which may ultimately lead to end-stage renal disease. Although the pathogenesis of diabetic nephropathy is multifactorial, mounting evidence indicates that inflammatory insults are among the cardinal pathogenic events implicated in the development and progression of the disease (1, 2). Accordingly, elevated levels of a wide variety of proinflammatory cytokines including TNF-α, IL-6, IL-1β, and the oxidative/proinflammatory transcription factor, nuclear factor-κB (NF-κB) as well as the chemokine, macrophage-chemoattractant protein-1 (*MCP-1*)/CC chemokine ligand-2, have been reported in diabetic nephropathy (1, 2). Moreover, NF-κB stimulates TNF-α, IL-6, IL-1β, and MCP-1 to potentiate macrophage infiltration in diabetic nephropathy (1, 3–6).

Macrophages express distinct patterns of surface receptors when responding to different stimuli (6, 7). It has become increasingly clear that macrophages exhibit two different polarization states known as classical or M1 phenotype and alternative or M2 phenotype (6, 7). The M1 phenotype stimulates inflammation, whereas the M2 phenotype is antiinflammatory (6, 7). Therefore, in diabetic nephropathy the high levels of chemokines, cytokines, and NF-κB would act in concert to enhance infiltration of the proinflammatory macrophage-M1 phenotype in tissues, creating a powerful inflammatory axis that would exacerbate tissue destruction. Similarly, the high inflammatory milieu created by NF-κB, TNF-α, IL-6, IL-1β, and MCP-1 would amplify renal fibrosis (1), a pathophysiological condition characterized by excessive accumulation of extracellular matrix and remodeling proteins such as collagen, fibronectin, and TGF-β1 that may eventually compromise kidney structure and function (8).

In patients with diabetic nephropathy, glomerular damage due to high deposits of extracellular matrix and elevated inflammatory insults increase the permeability of plasma proteins like albumin and transferrin, which are normally not freely filtered through the glomerulus, causing proteinuria (1, 2). Similarly, renal NF-κB activity has been correlated to the magnitude of proteinuria in patients with diabetic nephropathy (9). Thus, in diabetic nephropathy, the powerful inflammatory axis and elevated levels of extracellular matrix proteins would aggravate renal injury and kidney dysfunction. Therefore, the formulation of novel therapeutic modalities capable of selectively suppressing the proinflammatory macrophage-M1 phenotype, abating NF-κB, TNF-α, IL-6, IL-1β, and MCP-1 and suppressing extracellular matrix deposition while concomitantly enhancing the antiinflammatory macrophage-M2 phenotype would be useful to dampen renal inflammatory insults and thus preserve renal function and prevent or retard the progressive development of diabetic nephropathy to end-stage renal disease.

An important physiological cytoprotective pathway that could be explored against diabetic nephropathy is the heme-oxygenase (HO) system. HO is a microsomal enzyme that catalyzes the breakdown of the prooxidant heme to generate cytoprotective products including biliverdin/bilirubin, ferritin, and carbon monoxide to suppress oxidative stress/inflammation (6). HO has two main isoforms, which are inducible (HO-1) and constitutive (HO-2), whereas the third isoform, HO-3, is a pseudotranscript of HO-2, so HO activity is derived mainly from the HO-1 and HO-2 isoforms (6, 10–12). We recently reported the antidiabetic effects of the HO inducer, hemin, in different animal models including streptozotocin (STZ)-induced diabetic rats (13–18). However, the role of the HO system on macrophage polarization in renal dysfunction in STZ-induced type 1 diabetes has not been reported. Similarly, the effect of the HO system on macrophage infiltration in renal tissues of STZ diabetic animals remains largely unclear. Furthermore, the effects of the HO system on TNF-α, IL-6, and IL-1β in the kidney of STZ-diabetic animals have not been reported. Therefore, one of the main objectives of this study is to investigate the effects of the HO system on macrophage infiltration and to evaluate the expressions of the macrophage-M1 and -M2 phenotypes as well as to assess the levels of renal TNF-α, IL-6, IL1β, and kidney function in STZ-diabetic rats.

We recently showed that the mechanisms by which the HO system elicit cytoprotection, includes the potentiation of adiponectin, atrial natriuretic peptide (ANP), and its surrogate marker, urinary cGMP (18–20). Interestingly, ANP is also known to abate TNF-α, IL-6, and IL-1β (21), whereas adiponectin reportedly suppresses macrophage activation by abating NF-κB and TNF-α (22). However, no study has reported the effects of the HO system on renal ANP or kidney adiponectin in STZ-diabetic rats. Therefore, this study will evaluate the effects of the HO system on ANP and adiponectin in renal tissues from STZ-diabetic animals and correlate changes in ANP and adiponectin to the levels of NF-κB, TNF-α, IL-6, IL1β, MCP-1, and macrophage infiltration in STZ-diabetic animals. Besides suppressing inflammatory cytokines, ANP can also reduce fibrosis by inhibiting TGF-β1 and fibronectin (23). In contrast, aldosterone stimulates inflammation and fibrosis by activating NF-κB and activating-protein (AP-1) (24). Given that substances like TGF-β, fibronectin, aldosterone, NF-κB, and AP-1 are implicated in kidney dysfunction (8, 25), we will also measure these substances in renal tissues of STZ-diabetic animals and correlate the results to

proteinuria, albuminuria, creatinine clearance, and thus renal function.

In addition to MCP-1, another chemokine implicated in macrophage infiltration is the macrophage inflammatory protein-1α (MIP-1α) (26), also referred to as chemokine (C-C motif) ligand-3. Given that the role of MIP-1α in the kidneys of diabetic animals has not been reported, even though MIP-1α is an important chemokine endowed with powerful stimulatory effect on macrophage infiltration (26), we will also investigate the effects of the HO system on renal MIP-1α. Thus, this study will unveil novel mechanisms involved in the multifaceted role of the HO system against macrophage infiltration, proinflammatory chemokines/cytokines, and renal dysfunction in STZ-diabetic rats.

Materials and Methods (extended methodology is available in the Supplemental Data, published on The Endocrine Society's Journals Online web site at http://endo.endojournals.org)

Animals, treatment groups, and biochemical parameters

Our experimental protocol was approved by University of Saskatchewan Committee on Animal Care and Research Ethics and was in conformity with the Guide for Care and Usage of Laboratory Animals stipulated by the Canadian Council on Animal Care and the National Institutes of Health (National Institutes of Health publication number 85–23, revised 1996).

Male Sprague Dawley (SD) rats aged 7 weeks were purchased from Charles River Laboratory, housed at 21°C with 12-hour light, 12-hour dark cycles, fed with standard chow and had access to drinking water ad libitum. After a week of acclimatization, diabetes was induced with STZ (150 mg/kg · d, ip, in 0.1 mol/L citrate buffer, pH 4.5) as we previously reported (15). A week after STZ injection, the diabetic state was confirmed by the manifestation of polyuria, polydipsia, polyphagia, and elevated blood glucose (>20 mmol/L). To moderate the extent of the hyperglycemia and avoid the animals from dying, long-acting insulin (Lantus; Sanofi-Aventis) was administered sc (3 U/kg) three times weekly to all STZ-treated animals. Under these conditions glycemia did not exceed 26 mmol/L in the study groups. The diabetic animals were randomly divided into several experimental groups including (n = 6 per group): A, controls [1, normal SD; 2, SD treated with vehicle for STZ (citrate buffer); 3, SD treated with insulin]; B, STZ alone; C, STZ+hemin, the HO inducer; D, STZ+hemin+HO inhibitor, chromium-mesoporphyrin (CrMP); E, STZ+CrMP; and F, STZ+vehicle dissolving hemin and CrMP.

Hemin (30 mg/kg, ip; Sigma) and CrMP (4 μmol/kg, ip, Porphyrin Products) were previously reported and administered three times weekly for 8 weeks (8, 16, 27–31). Although many HO inhibitors are nonspecific and may affects other hemoenzymes or even increase HO-1 expression (32), however, CrMP administered at a dose of 4 μmol/kg is reportedly selectively against HO activity (33).

During the treatment period, fasting glucose was measured on a weekly basis by means of a glucose meter (BD Biosciences). Systolic blood pressure (BP) was measured by noninvasive tail-cuff method (model 29 SSP; Harvard Apparatus). At least six different readings were taken to calculate the mean systolic BP. Prior to killing, the animals were placed in metabolic cages for 24 hours with free access to food and water, and urine was collected and measured. Subsequently the animals were weighed, anesthetized with pentobarbital sodium (50 mg/kg body weight) and plasma, and the kidney collected. Kidney hypertrophy was determined by the kidney to body weight ratio, an index of kidney hypertrophy (8), whereas plasma creatinine, sodium and urine (sodium, proteinuria, albuminuria and creatinine), and creatinine clearance were analyzed as previously reported (8).

HO activity was determined by spectrophotometric assay as we previously reported (8, 19), whereas an ELISA was used for HO-1 (Stressgen-Assay Design), TNF-β, IL-6,and IL-1β (Immuno-Biological Laboratories Co Ltd), MCP-1 and MIP-1α (OmniKine; Assay Biotechnology Co Inc), and adiponectin (Pharmaceuticals, Inc) and an enzyme immunoassay for cGMP and aldosterone (Cayman Chemical), as we previously reported (27, 29, 34).

Histological and morphological analyses of the kidneys

Histological and morphological analyses were done as we previously described (13). The kidney was fixed in 10% formalin, processed, and paraffin embedded, and then whole sections of 5 μm were cut and stained with hematoxylin and eosin and examined using a virtual microscope (Aperio Scan Scope model CS; Aperio Technology Inc). Morphological assessment was done by randomly taking 20 snapshots per slide per group of four to six animals (80–120 images per group). The images were analyzed using an Aperio Image Scope version 11.2.0.780 software (Aperio; e-Pathology Solution) and subsequently scored semiquantitatively by a blinded researcher, as we previously reported (13, 35).

Western immunoblotting

The kidney was homogenized in the presence of a cocktail of protease inhibitors as we previously described (28, 29) with primary antibodies [Santa Cruz Biotechnology; fibronectin (sc-18825), collagen-IV (sc-11360), TGF-β1/2/3 (sc7892), ED-1 (CD68) (sc-59103), ED-2 (CD163) (sc-58956), IL-10 (sc-52561)], NF-κB (Chemicon International Inc), AP-1 (Abcam Inc), and phosphorylated AMP-activated protein kinase (AMPK; Cell Signaling Technology Inc). After scanning the bands of the blots, densitometric analyses were carried out using UN-SCAN-IT software (Silk Scientific). β-Actin (Sigma) was used as a control to ascertain equivalent loading.

Total RNA isolation and quantitative real-time RT-PCR

The kidney was homogenized in 0.5 mL Trizol reagent (Invitrogen Life Technologies) and reverse transcription carried out using a first-strand cDNA synthesis kit (Novagen), as we previously reported (8, 28). Quantitative PCR was performed with Applied Biosystems 7300 Real-Time PCR system and iQ SYBR Green supermix (Bio-Rad Lab-

oratories). Triplicate samples containing 1 μL of cDNA were run using a template of 3.2 pmol of primers for (p65-NF-κB) (forward, 5′-CATGCGTTTCCGTTACAAGTGCGA-3′, and reverse, 5′-TGGGTGCGTCTTAGTGGTATCTGT-3′); AP-1 (forward, 5′-AGCAGATGCTTGAGTTGAGAGCCA-3′ and reverse, 5′-TTCCATGGGTCCCTGCTTTGAGAT-3′); and β-actin (forward, 5′-TCATCACTATCGGCAATGAGCGGT-3′, and reverse, 5′-ACAGCACTGTGTTGGCATAGAGGT-3′) in a final volume of 25 μL, as we previously reported (8, 28).

Statistical analyses

All data are expressed as means ± SEM from at least four independent experiments unless otherwise stated. Statistical analyses (parametric and nonparametric where appropriate) were done using a two-way ANOVA, using Statistical Analysis System software, version 9.3 (SAS Institute Inc) and a Student's *t* test. Group differences at the level of $P < .05$ were considered statistically significant.

Results

Hemin potentiated HO, reduced hyperglycemia, and abated aldosterone, NF-κB, and AP-1

The administration of hemin therapy to STZ-diabetic rats lowered fasting blood glucose from 23.4 ± 1.3 mmol/L to 10.8 ± 0.9 mmol/L, $P < .01$ (Table 1). In contrast, coadministering the HO inducer, hemin, together with the HO inhibitor, CrMP abolished the antidiabetic effect of hemin (23.4 ± 1.3 mmol/L vs 21.3 ± 2.7 mmol/L), whereas treatment with CrMP alone exacerbated hyperglycemia (25.7 ± 1.8 mmol/L) (Table 1). The hemin-dependent reduction of hyperglycemia was accompanied by significant enhancement of HO-1 and HO activity in STZ-diabetic rats by 2.7- and 4.5-fold, respectively (Figure 1, A and B). Although the basal HO-1 in STZ-diabetic rats was slightly but significantly higher than the levels in the control-SD rats, it did not evoke any changes in HO activity, suggesting it that might have been below the necessary threshold necessary to trigger an increase in HO activity.

Because STZ diabetes is characterized by elevated inflammation and increased production of aldosterone (36), a hormone that trigger inflammatory insults by activating NF-κB and AP-1 (24) in addition to its traditional role in regulating sodium/water retention, we investigated the effects of up-regulating the HO system with hemin on kidney and urinary aldosterone. Interestingly, hemin therapy markedly reduced the elevated levels of aldosterone in the kidney and in urine by 2.5- and 2.1-fold, respectively (Figure 1, C and D), whereas cotreatment with the HO inhibitor CrMP nullified the effects of hemin, whereas treatment with CrMP alone further enhanced the levels of

Table 1. Effect of Hemin and CrMP on Physiological Variables in STZ-Diabetic Rats

	Animal Groups							
	Controls							
Physiological Variables	Normal SD	SD + Vehicle for STZ	SD + Insulin (Sub therapeutic Dose)	STZ	STZ + Hemin	STZ + Hemin + CrMP	STZ + CrMP	STZ + Vehicle for Hemin and CrMP
Body weight, g	384.6 ± 6.3	375.9 ± 5.4	381.9 ± 7.8	314.6 ± 10.8[a]	307.5 ± 9.2[a]	301.8 ± 9.4[a]	310.4 ± 11.3[a]	305.5 ± 7.5[a]
Fasting glucose, mmol/L	7.1 ± 0.4	7.4 ± 0.3	7.0 ± 0.5	23.4 ± 1.3[b]	10.8 ± 0.9[c]	21.3 ± 2.7[d]	25.7 ± 1.8	24.5 ± 1.2
Kidney hypertrophy, g/kg body weight	3.1 ± 0.5	2.8 ± 0.4	2.6 ± 0.3	5.8 ± 0.6[e]	3.9 ± 0.7[c]	6.2 ± 1.2[d]	7.1 ± 1.3	5.5 ± 1.2
Systolic BP, mm Hg	119.7 ± 1.8	125.3 ± 3.4	118.7 ± 2.9	130.4 ± 2.5[e]	120.8 ± 2.2[c]	128.9 ± 1.7	139.3 ± 1.5	132.4 ± 2.1
Water intake, mL per 24 h	46.3 ± 3.7	43.9 ± 5.1	47.1 ± 8.7	243.2 ± 9.4[b]	175.8 ± 7.1[d]	237.9 ± 12.6	258.5 ± 9.3	249.5 ± 11.3
Urine volume, mL per 24 h	30.5 ± 7.3	34.7 ± 8.5	32.5 ± 11.2	196.3 ± 13.8[b]	254.2 ± 10.6[d]	189.5 ± 9.4	176.4 ± 14.9	207.3 ± 12.5
Albuminuria, mg per 24 h	2.1 ± 0.3	2.4 ± 0.2	2.2 ± 0.4	52.7 ± 2.5[b]	12.3 ± 1.8[d]	61.7 ± 5.3	71.5 ± 4.7	57.6 ± 5.9
Proteinuria, mg per 24 h	8.6 ± 0.8	9.1 ± 1.1	8.9 ± 1.3	105.3 ± 7.4[b]	20.5 ± 2.4[d]	97.6 ± 5.3	124.7 ± 5.2	112. ± 10.7
Plasma sodium, mmol/L	136.7 ± 2.3	139.2 ± 1.6	135.6 ± 1.8	152.3 ± 3.4[e]	140.5 ± 1.6[c]	154.9 ± 2.9	162.3 ± 3.7	155.6 ± 3.5
Urinary sodium, mmol/L	131.2 ± 1.8	133.1 ± 1.7	132.8 ± 2.2	122.5 ± 1.5[e]	137.5 ± 2.1[c]	123.6 ± 1.8	120.4 ± 2.3	121.3 ± 1.9
Creatinine clearance, ml/min · g kidney	4.9 ± 0.5	4.7 ± 0.4	4.8 ± 0.6	3.2 ± 0.3[e]	4.1 ± 0.4[c]	3.3 ± 0.5	2.9 ± 0.1	3.4 ± 0.3

[a] $P < .05$ vs normal SD or SD+insulin or SD+vehicle for STZ.
[b] $P < .01$ vs normal SD or SD+insulin or SD+vehicle for STZ.
[c] $P < .05$ vs STZ or STZ+hemin+CrMP or STZ+CrMP or STZ+vehicle for hemin/CrMP.
[d] $P < .01$ vs STZ or STZ+hemin+CrMP or STZ+CrMP or STZ+vehicle for hemin/CrMP.
[e] $P < .05$ vs normal SD or SD+insulin or SD+vehicle for STZ.

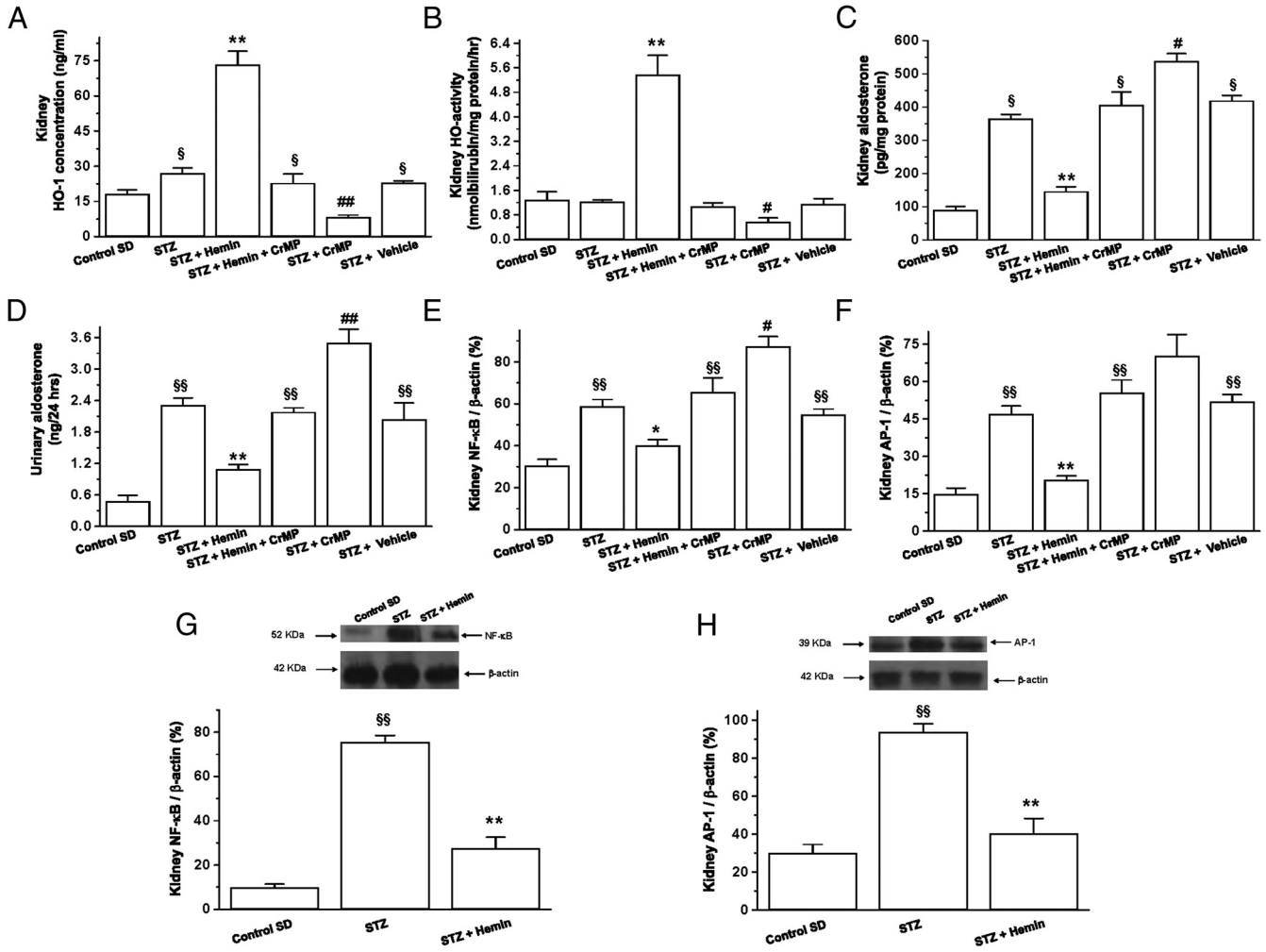

Figure 1. Effects of the HO inducer hemin and the HO inhibitor CrMP on kidney HO-1, HO activity, aldosterone, NF-κB, and AP-1 in STZ-diabetic rats. A, The basal HO-1 levels in STZ-diabetic rats were higher than control-SD rats. Hemin therapy markedly increased HO-1 concentration, whereas the HO blocker of CrMP annulled the hemin effect. B, Hemin therapy robustly enhanced HO activity in STZ-diabetic rats, whereas the HO blocker CrMP annulled the effects of hemin. C, Hemin therapy significantly depleted the elevated basal levels of kidney aldosterone in STZ-diabetic rats, whereas the HO blocker CrMP nullified the effects of hemin. D, Hemin therapy markedly reduced the elevated basal levels of urinary aldosterone in STZ-diabetic rats, whereas the HO blocker CrMP abolished the effects of hemin. Quantitative real-time RT-PCR indicated that hemin therapy abrogated the elevated basal mRNA expression of NF-κB (E) and AP-1 (F) in the kidney of STZ-diabetic rats, but CrMP reversed and exacerbated the hemin effect, with a further increase in the levels of NF-κB and AP-1. Representative Western immunoblots and relative densitometry of expressed proteins indicates the basal expressions of NF-κB (G) and AP-1 (H) were significantly elevated in STZ-diabetic rats as compared with control-SD but were reduced by hemin therapy. The vehicle dissolving hemin and CrMP had no effect on HO-1, HO activity, kidney aldosterone, urinary aldosterone, and the mRNA expression of NF-κB and AP-1. Bars represent means ± SEM (n = 6 rats per group). *, $P < .05$, **, $P < .01$ vs STZ; §, $P < .05$, §§, $P < .01$ vs control-SD; #, $P < .05$, ##, $P < .01$ vs STZ or STZ+hemin+CrMP, or STZ+vehicle.

aldosterone. Similarly, hemin therapy significantly abated the elevated levels of oxidative/inflammatory transcription factors in the kidney such as NF-κB and AP-1 (Figure 1, E and F). On the other hand, the administration of the HO-inhibitor with hemin or alone nullified the hemin effect and increased NF-κB and AP-1 in STZ-diabetic rats. To ascertain that the hemin-induced suppression of NF-κB and AP-1 mRNA expressions were accompanied by a parallel reduction of the corresponding proteins, we used Western immunoblotting to measure the protein expressions of NF-κB and AP-1 in the kidneys (Figure 1, G and H). Our Western immunoblot and relative quantitative analyses of the expressed proteins normalized by β-actin indicated that the basal expressions of NF-κB and AP-1 in STZ-diabetic animals were significantly elevated by 7.6- and 3.1-fold, respectively, as compared with the SD-controls (Figure 1, G and H). Treatment with hemin reduced the protein expressions of NF-κB and AP-1 by 2.6- and 2.3-fold, respectively, suggesting that hemin concomitantly reduced both the mRNA and protein expressions of NF-κB and AP-1 in STZ-diabetic rats.

We also measured water intake because aldosterone favors sodium/water retention and diabetes is generally associated with increased water intake. In STZ-diabetic

animals the elevated levels of aldosterone was accompanied by greater water intake (Table 1). Accordingly, water intake in STZ-diabetic rats was 243.2 ± 9.4 mL per 24 hours, whereas in hemin-treated STZ animals, water intake was significantly reduced to 175.8 ± 7.1 mL per 24 hours. On the other hand, treatment with the HO inhibitor CrMP nullified the effects of hemin and increased the water intake to 258.5 ± 9.3 mL per 24 hours. Because hemin therapy suppressed the levels of aldosterone and correspondingly reduced water intake, we also evaluated the effect of hemin on plasma sodium. In the STZ-diabetic rats, plasma sodium retention was significantly elevated as compared with the control rats (Table 1) but was reduced by hemin therapy, whereas the HO inhibitor CrMP abolished the effects of hemin and exacerbated the levels of plasma sodium. The hemin-dependent reduction of plasma sodium was accompanied by an increased excretion of urinary sodium (Table 1), whereas treatment with the HO inhibitor nullified the effects of hemin.

Because renal damage is associated with hypertrophy (8, 19), we used the organ-to-body weight index to establish hypertrophy (8, 19). Our results indicate that hemin therapy attenuated kidney hypertrophy in STZ-diabetic rats, and this effect was abolished by the HO inhibitor CrMP (Table 1). To further confirm renal damage in the STZ-diabetic rats, we measured important clinical indices of renal function including albuminuria, proteinuria, and creatinine clearance and detected significantly elevated levels of proteinuria and albuminuria in STZ-diabetic rats that were accompanied by significant reduction of creatinine clearance, thus suggesting renal dysfunction (Table 1). These renal defects were reversed by hemin therapy, whereas cotreatment with CrMP or treatment with CrMP alone abolished the renoprotective effects of hemin with aggravation of albuminuria, proteinuria, and creatinine clearance in STZ-diabetic rats.

Because we observed increased aldosterone levels and elevated water retention in STZ-diabetic rats, we measured systolic BP. However, BP was normotensive in all treatment groups, although it was 5 mm Hg higher in the STZ-diabetic rats. Treatment with hemin slightly lowered BP, whereas CrMP abolished the modest effect (Table 1).

The application of STZ injection to induce diabetes caused reduction in body weight. STZ is well known to cause loss of body weight and/or retard growth (37, 38), so the loss of body weight by STZ was expected. On the other hand, the administration of hemin, hemin+CrMP, CrMP alone, or the vehicle dissolving hemin and CrMP further reduced body weight slightly as compared with STZ-diabetic rats. A difference (<5%) was observed (Table 1). Accordingly, in STZ+hemin, STZ+hemin+CrMP, STZ+CrMP, and STZ+vehicle for hemin/CrMP groups, the body weights were lower by 2.2%, 4.1%, 1.3%, and 3%, respectively, as compared with the STZ-diabetic animals. Although loss of body weight can affect glycemic levels, it is unlikely in this situation because the slight loss of body weight in hemin- and CrMP-treated animals were accompanied by opposite glycemic effects (Table 1) because we observed a slight decrease of glucose levels in hemin-treated animals but a small increase in CrMP-treated animals, suggesting that the HO system may be endowed with intrinsic antidiabetic effects. The mild subtherapeutic dose of insulin of 3 U/kg or the vehicle for STZ (citrate buffer, pH 4.5) or the vehicle dissolving hemin and CrMP (0.1 M NaOH, titrated to pH 7.4 with 0.1 M HCl in PBS) did not affect any of the measured parameters (Table 1).

Hemin therapy enhanced ANP and its surrogate marker, urinary cGMP

Given that ANP is potentiated by the HO system (19) and that both ANP and the HO system have antiinflammatory properties (6, 21) and promotes natriuresis (39, 40), we investigated whether the concomitant potentiation of the HO system and ANP by hemin therapy would abate macrophage-infiltration and increase the excretion of urinary sodium. In STZ-diabetic rats, the basal levels of plasma and renal ANP were slightly but significantly higher than in the control-SD rats (Figure 2). Treatment with hemin greatly enhanced plasma and renal ANP by 3.1- and 2.9-fold, respectively, and correspondingly enhanced the excretion of urinary sodium (Table 1), whereas the coadministration of the HO inducer, hemin, together with the HO inhibitor, CrMP, nullified the effects of hemin, whereas treatment with CrMP alone resulted in further depletion of the levels of ANP (Figure 2, A and B). We also measured urinary cGMP, a surrogate marker of ANP (41). Although the basal levels of ANP in STZ-diabetic rats were higher than control-SD, the levels of urinary cGMP, a secondary messenger through which ANP elicits is effects (39), were significantly depressed by 2.1-fold in STZ-diabetic rats (Figure 2C). Treatment with hemin greatly enhanced urinary cGMP by 3.5-fold, whereas cotreatment with CrMP nullified the effects and CrMP alone abrogated the basal levels of urinary cGMP in STZ-diabetic rats.

Hemin therapy enhanced adiponectin and AMPK in STZ-diabetic rats

Given that the HO system is known to potentiate adiponectin (21, 42) and adiponectin is an antiinflammatory protein (22) with renoprotective effects (43), we investigated the effects of hemin therapy on adiponectin. In STZ-diabetic rats, plasma and renal adiponectin were markedly

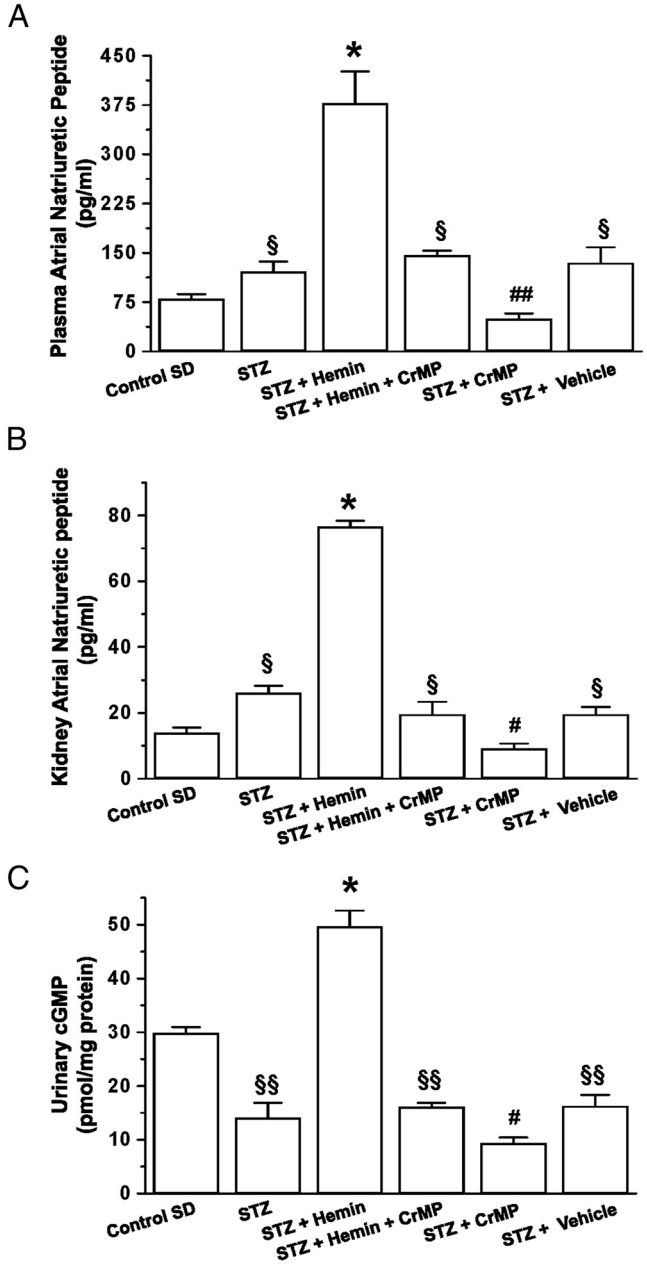

Figure 2. Effects of the HO inducer hemin and the HO inhibitor CrMP on ANP and urinary cGMP in STZ-diabetic rats. The basal levels of plasma ANP (A) and kidney ANP (B) in STZ-diabetic rats were slightly higher than in the control-SD rats but were markedly enhanced by hemin, whereas the HO blocker CrMP annulled the hemin effect. C, Hemin therapy significantly increased urinary cGMP, a surrogate marker of ANP, but the HO inhibitor CrMP annulled the effects of hemin. The vehicle dissolving hemin and CrMP had no effect on plasma ANP, kidney ANP, and urinary GMP. Bars represent means ± SEM (n = 6 rats per group). *, $P < .01$ vs STZ; §, $P < .05$, §§, $P < .01$ vs control-SD; #, $P < .05$, ##, $P < .01$ vs STZ or STZ+hemin+CrMP or STZ+vehicle.

reduced (Figure 3, A and B) by 3.2- and 2.1-fold, respectively. However, hemin therapy greatly enhanced the depressed levels of adiponectin in the plasma and kidney by 3.6- and 1.8-fold, respectively, whereas the coapplication of the HO blocker CrMP together with hemin nullified the hemin-induced increase, whereas CrMP alone further reduced the levels of basal adiponectin in plasma and the kidney (Figure 3, A and B).

Because the effects of adiponectin are mediated via AMPK (44), we investigated whether the hemin-induced increase of adiponectin will be accompanied by a corresponding increase of AMPK. Our results indicate that hemin therapy robustly enhanced the AMPK expression in the STZ-diabetic rats to comparable levels as in the control-SD animals (Figure 3C).

Hemin therapy suppressed proinflammatory cytokines in STZ-diabetic rats

Because TNF-α, IL-6, and IL-1β are proinflammatory cytokines that impair renal function (1, 2) and ANP and an up-regulated HO-system are known to suppress TNF-α, IL-6, and IL-1β (21, 42) in addition to promoting natriuresis (39), we investigated the effects of concomitantly enhancing ANP and the HO system with hemin therapy on these cytokines. In STZ-diabetic rats, the levels of urinary and kidney TNF-α, IL-6, and IL-1β were markedly elevated as compared with control-SD rats (Figure 4, A–F). Interestingly, the administration of hemin to STZ-diabetic rats significantly abated the elevated levels of kidney TNF-α, IL-6, and IL-1β by 1.9-, 2.7-, and 3-fold, respectively, although similar levels as observed in control-SD rats were not attained. Similarly, urinary TNF-α, IL-6, and IL-1β were abrogated by 3.1-, 3.4-, and 2.6-fold, respectively, albeit the levels as in control-SD were not reinstated. Interestingly, the suppression of TNF-α coincided with reduced plasma sodium (Table 1) and because TNF-α is known to enhance sodium uptake in the distal renal tubule by stimulating epithelial sodium channels (45, 46), the hemin-dependent reduction of TNF-α may account for reduced plasma sodium (Table 1).

On the other hand, the coadministration of the HO blocker CrMP and the HO inducer hemin abolished the effects of hemin, whereas treatment with CrMP alone exacerbated the levels of urinary and kidney TNF-α, IL-6, and IL-1β (Figure 4, A–F). The vehicle dissolving hemin and CrMP had no effect on urinary and kidney TNF-α, IL-6, and IL-1β.

Hemin therapy suppressed proinflammatory chemokines in STZ-diabetic rats

MIP-1α and MCP-1 are two potent chomokines implicated in macrophage infiltration (26, 47, 48), so we investigated the effects of hemin therapy on MIP-1α and MCP-1. In STZ-diabetic rats, the levels of urinary and kidney MCP-1 were significantly elevated by 2.5- and 2.8-fold, respectively (Figure 5, A and B). However, treatment with hemin greatly attenuated the elevated levels of uri-

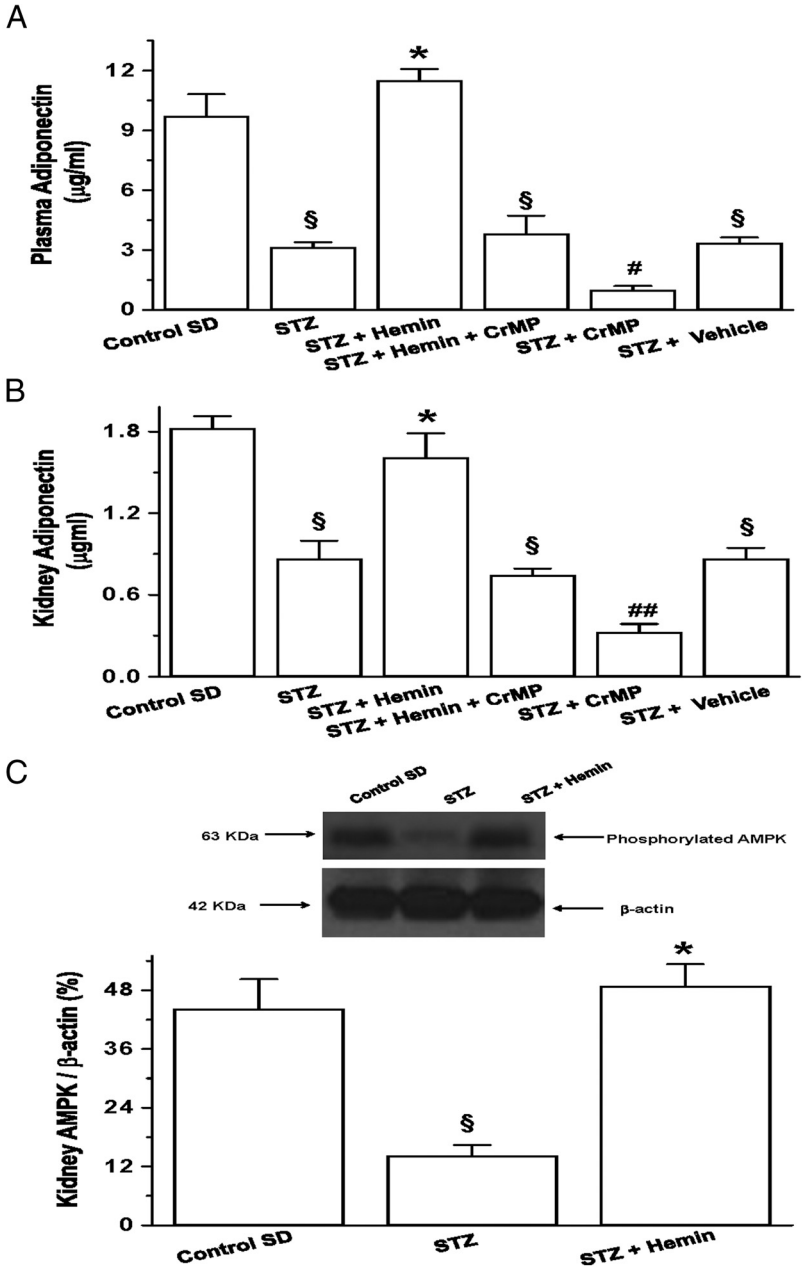

Figure 3. Effects of the HO inducer hemin and the HO inhibitor CrMP on adiponectin and AMPK in STZ-diabetic rats. The basal levels of plasma adiponectin (A) and kidney adiponectin (B) in STZ-diabetic rats were significantly lower than in the control-SD rats but were greatly increased by hemin, whereas the HO blocker CrMP nullified the hemin effect. The vehicle dissolving hemin and CrMP had no effect on plasma and kidney adiponectin levels. C, Representative Western immunoblotting and relative densitometry indicates that the basal expression of AMPK in STZ-diabetic rats was markedly reduced; however, treatment with hemin significantly increased the expression of AMPK. Bars represent means ± SEM (n = 4–6 rats per group). *, $P < .01$ vs STZ; §, $P < .01$ vs control-SD; #, $P < .05$, ##, $P < .01$ vs STZ or STZ+hemin+CrMP or STZ+vehicle.

nary and kidneys MCP-1 by 2.1- and 1.8-fold, respectively, whereas the coapplication of the HO inducer hemin and the HO inhibitor CrMP abolished the hemin effects and restored similar levels of urinary and renal MCP-1 as in the STZ-diabetic animals. On the other hand, treatment with CrMP alone resulted in further accentuation in the levels of urinary and kidneys MCP-1 (Figure 5, A and B). Although hemin therapy did not restore the levels of MCP-1 in the kidney of the STZ-diabetic animals to similar levels as in the control-SD animals, however, hemin therapy effectively abrogated the excessive levels of urinary MCP-1 to comparable levels as in the control-SD rat (Figure 5, A and 5B).

Hemin therapy was also effective against MIP-1α. In STZ-diabetic rats, the basal MIP-1α levels in the kidney was significantly elevated by 3.5-fold but was abated by hemin to comparable levels as in the control-SD rats, whereas coadministration of hemin with CrMP abolished the hemin-dependent reduction of MIP-1α, whereas treatment with CrMP alone triggered further increase in MIP-1α (Figure 5C).

Hemin therapy selectively enhanced the antiinflammatory macrophage M2 phenotype but abated the proinflammatory M1 phenotype and interstitial macrophage infiltration

After having observed the hemin-dependent suppression of chemokines like MIP-1α and MCP-1, which are implicated in macrophage infiltration, we used specific markers such as ED1 (activated macrophage) to quantify the proinflammatory M1 phenotype and ED2 and IL-10 for the assessment of the antiinflammatory M2 phenotype (49, 50). Interestingly, our Western immunoblotting and relative densitometric analyses revealed that basal expression of ED1 in STZ-diabetic animals was markedly elevated by 5.1-fold as compared with the control-SD (Figure 6A). However, the administration of hemin therapy significantly reduced the elevated expression of the proinflammatory M1 phenotype marker ED1 in the kidney of STZ-diabetic animals. Interestingly, the hemin-dependent abrogation of ED1 was accompanied by the enhancement of the depressed and aberrant expression of the basal antiinflam-

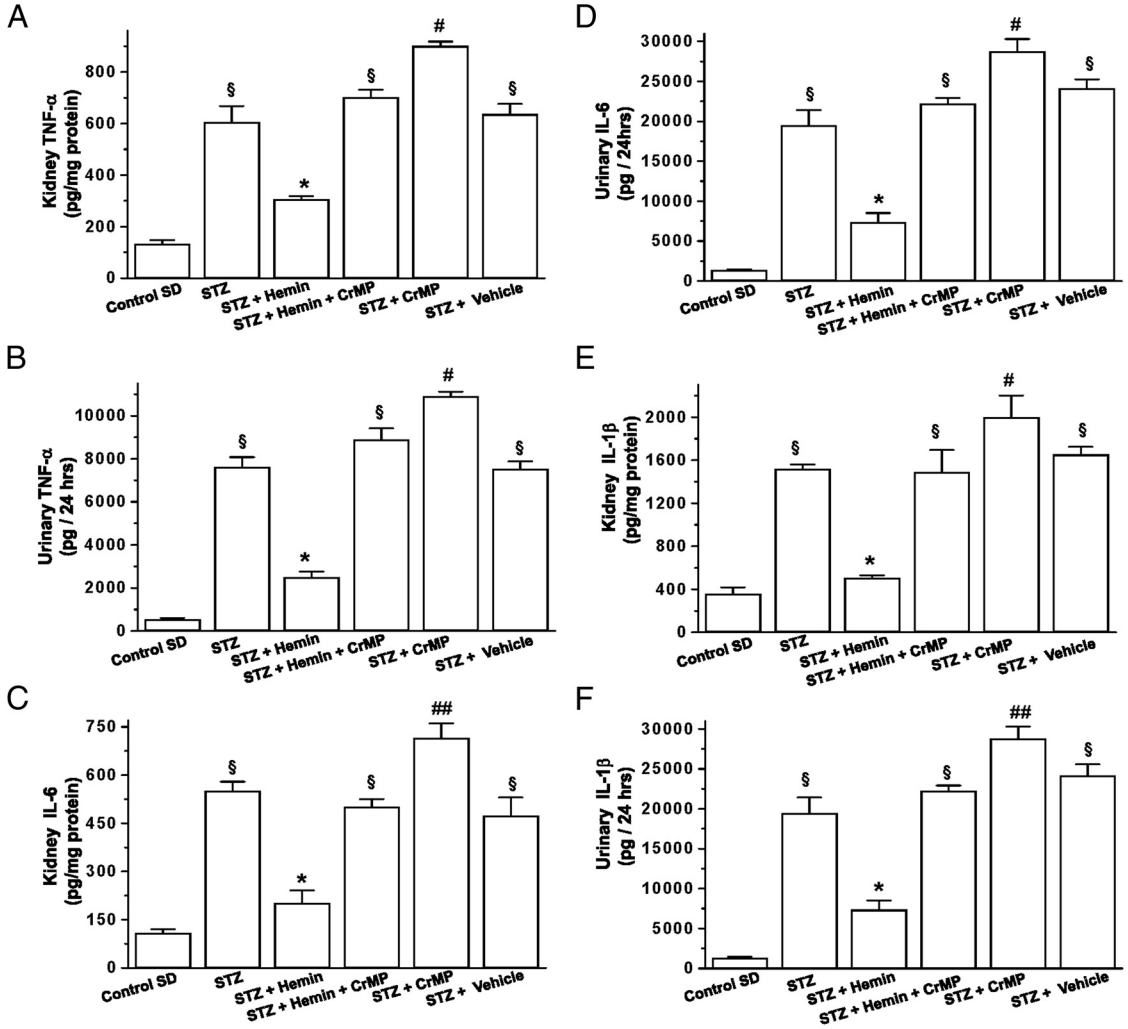

Figure 4. Effects of the HO inducer hemin and the HO inhibitor CrMP on kidney and urinary TNF-α, IL-6, and IL-1β in STZ-diabetic rats. The basal levels of kidney TNF-α (A), urinary TNF-α (B), kidney IL-6 (C), urinary IL-6 (D), kidney IL-1β (E), and urinary IL-1β (F) in STZ-diabetic rats were significantly higher than the levels in control-SD rats but were markedly attenuated by hemin therapy, whereas the HO blocker CrMP annulled the hemin effect, with further increase in the levels of TNF-α, IL-6, and IL-1β. The vehicle dissolving hemin and CrMP had no effect on plasma or urinary TNF-α, IL-6, and IL1β. Bars represent means $\pm$ SEM (n = 6 rats per group). *, $P < .01$ vs STZ; §, $P < .01$ vs control-SD; #, $P < .05$, ##, $P < .01$ vs STZ or STZ+hemin+CrMP or STZ+vehicle.

matory M2 phenotype (Figure 6, B and C). Accordingly, hemin therapy robustly enhanced important markers of the M2 phenotype such as ED2 (Figure 6B) and IL-10 (Figure 6C) by 4.8- and 3.9-fold, respectively, suggesting that hemin may selectively modulate the polarization of the macrophage toward the M2 phenotype that attenuates inflammatory insults.

To further evaluate the effects of hemin on macrophage infiltration and renal lesions, we used histology and morphological analyses to evaluate interstitial macrophage infiltration in renal sections (Figure 6C). Our histology data revealed increased interstitial macrophage infiltration in STZ-diabetic animals as compared with the control-SD rats (Figure 6C), which was interestingly reduced by hemin. The reduction of interstitial macrophage infiltration in hemin-treated STZ was further confirmed by semiquantitative morphological analyses (Figure 6D).

Hemin therapy suppressed extracellular matrix and profibrotic proteins

Because elevated deposition of extracellular matrix and increased inflammatory events are pathophysiological factors that destroy the glomerulus causing proteinuria (1, 2) and ANP and adiponectin are known to protect renal tissue (43, 51) by suppressing fibrosis caused by the deposition of extracellular matrix (23, 52), we investigated whether the concomitant potentiation of ANP, adiponectin, and the HO system by the hemin would suppress TGF-β, a profibrotic protein implicated renal injury and proteinuria (53). In STZ-dia-

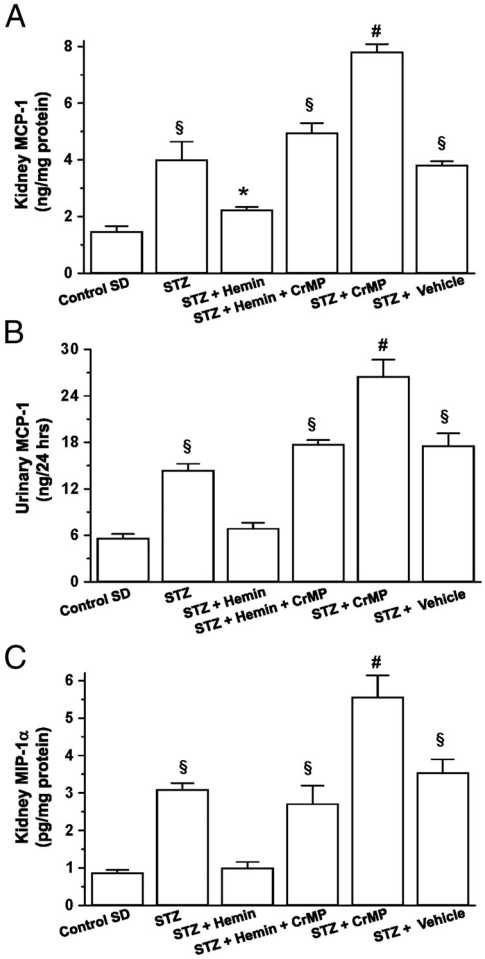

Figure 5. Effects of the HO inducer, hemin and the HO inhibitor CrMP on kidney and urinary *MCP-1* and MIP-1α in STZ-diabetic rats. The basal levels of kidney MCP-1 (A), urinary MCP-1 (B), and kidney MIP-1α (C) in STZ-diabetic rats were significantly elevated as compared with the levels in control-SD rats, but hemin therapy greatly suppressed the elevated levels of MIP-1α and MCP-1, whereas the HO blocker CrMP annulled the hemin effect, with a further increase in the levels of MIP-1α and MCP-1. The vehicle dissolving hemin and CrMP had no effect on kidney or urinary of MIP-1α and MCP-1. Bars represent means ± SEM (n = 6 rats per group). *, $P < .01$ vs STZ; §, $P < .01$ vs control-SD; #, $P < .01$ vs STZ or STZ+hemin+CrMP or STZ+vehicle.

betic animals, renal insufficiency was accompanied by marked elevation of the basal expression of TGF-β (Figure 7A). We observed a 3.9-fold increase of TGF-β in STZ-diabetic animals.

Given that TGF-β mobilizes the extracellular matrix by stimulating fibronectin and collagen to cause fibrosis and proteinuria (53), we also investigated the effects of hemin therapy on the expressions of fibronectin and collagen-IV (Figure 7, B and C). In STZ-diabetic rats, the basal expressions of fibronectin and collagen-IV were markedly elevated by 2.9- and 3.4-fold, respectively, as compared with control-SD rats. However, hemin therapy greatly suppressed the levels of fibronectin and collagen-IV (Figure 7, B and C). Hemin therapy was more effective against collagen-IV because control levels were reinstated. Because elevated extracellular matrix/profibrotic proteins such as TGF-β, fibronectin, and collagen are implicated in renal lesions (8), we investigated whether the hemin-dependent suppression of these profibrotic proteins would improve kidney injury in STZ. Our results indicate that kidney section from control-SD showed no signs of pathology in the cortex and the medulla; however, mild congestion in some kidney sections was noted (Figure 7D). In contrast, the STZ-diabetic animals displayed severe morphological kidney lesions such as interstitial macrophage infiltration, glomerulosclerosis, tubular necrosis, intertubular/perivascular fibrosis, tubular vacuolization, deposition of hyaline/tubular cast, and tubular and glomerular necrosis. Interestingly, in hemin-treated STZ, there was marked reduction of glomerulosclerosis, hyaline/tubular cast formations, and tubular vacuolization (Figure 7D). These observations were further confirmed by semiquantitative morphological analyses showing that hemin significantly abated renal lesions (Figure 7E).

Discussion

The accumulation of macrophages in tissues of diabetic patients is a cardinal feature in the progression and development of diabetic nephropathy. Strong evidence from cell-depletion studies in animals has demonstrated the pathophysiological role of macrophages and their contribution in exacerbating inflammatory cascades in the kidneys of diabetic patients (1). The present study demonstrates that hemin therapy is a potent renoprotective agent against STZ-induced type 1 diabetes. In this model, excessive macrophage infiltration alongside the elevated levels of NF-κB, TNF-α, IL-6, IL-1β, aldosterone, TGF-β, and extracellular matrix deposition are among the complex molecular processes that characterize the intricate relationship between inflammation, renal fibrosis, and the development and progression of diabetic nephropathy (1–6, 8, 9, 54). Importantly, our study unveils for the first time that hemin therapy selectively enhance the antiinflammatory macrophage M2 phenotype in STZ-diabetic rats while concomitantly abating the proinflammatory M1 phenotype, suggesting that a novel mechanism by which hemin therapy counteracts renal inflammation in type 1 diabetes is by selectively favoring the polarization of macrophage toward the M2 phenotype that dampens inflammation. Correspondingly, hemin therapy abated chemokines that promote macrophage infiltration such as MIP-1α and MCP-1 (1, 2, 26). The effect of hemin therapy on MIP-1α in STZ-diabetic rat is novel observation reported

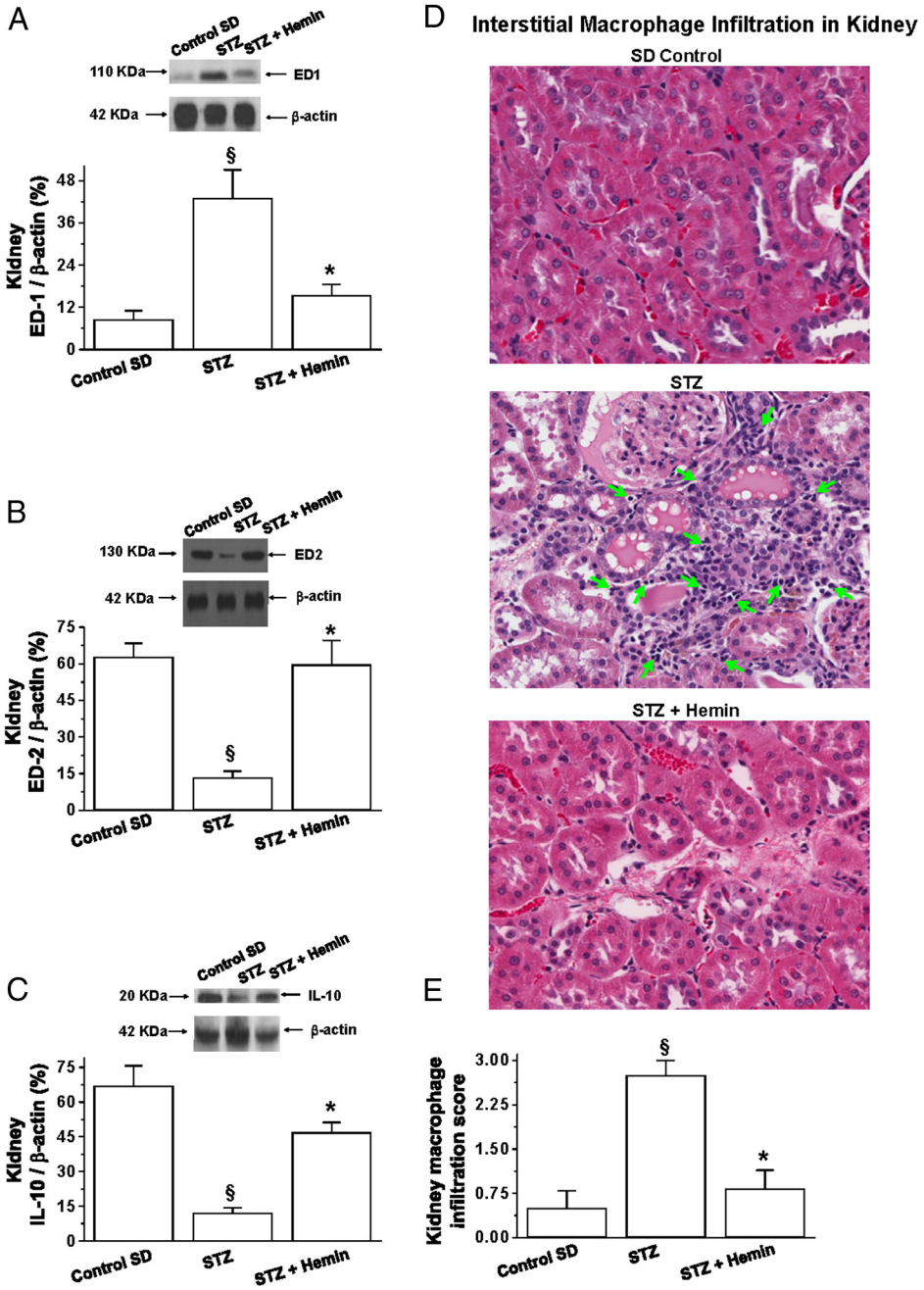

Figure 6. Effect of hemin therapy on macrophage M1 phenotype and M2 phenotype in the kidney of STZ-diabetic rats. A, Representative Western immunoblots and relative densitometry indicates the basal expression of ED1, the proinflammatory M1 phenotype marker, was markedly elevated in STZ-diabetic rats as compared with control-SD but was significantly reduced by hemin therapy. Representative Western immunoblottings and relative densitometric analyses revealed that the basal expression of ED2 (B) and IL-10 (C), two important antiinflammatory M2 phenotype markers, were greatly reduced in STZ-diabetic rats as compared with nondiabetic SD-control but were significantly enhanced by hemin therapy to comparable levels as observed in the control-SD rats. D, Representative images of histopathological lesions of kidney sections. Images from control-SD had very little interstitial macrophage infiltration. However, in STZ-diabetic animals, there was abundant macrophage infiltration but was reduced by hemin therapy. Magnification, ×200. E, Semiquantitative morphological evaluation showed that hemin therapy significantly abated macrophage infiltration. Arrows indicate areas with abundant interstitial macrophages. Bars represent means ± SEM (n = 4–6 rats per group). *, $P < .01$ vs STZ; §, $P < .01$ vs control-SD.

here for the first time. Importantly, the hemin-dependent suppression of inflammatory mediators in STZ-diabetic animals was associated with the parallel reduction of several renal lesions including glomerulosclerosis, tubular vacuolization, intertubular/perivascular fibrosis, deposition of hyaline/tubular cast, tubular/glomerular necrosism and interstitial macrophage infiltration.

Another intriguing observation from our study is the hemin-dependent potentiation of ANP, a substance known to cause natriuresis. Therefore, the increased so-

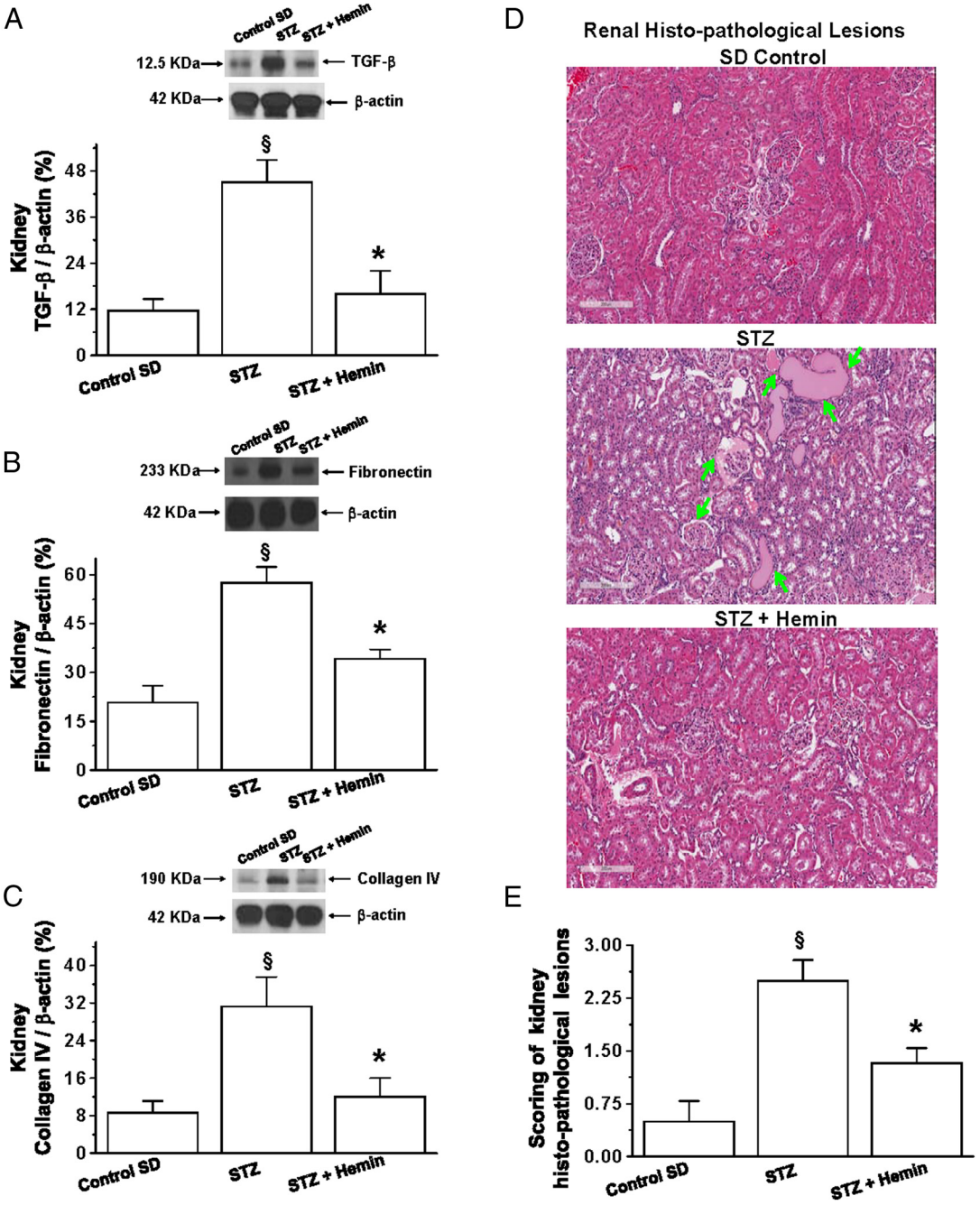

Figure 7. Effect of hemin therapy on the expression of transforming growth factor-beta (TGF-β), fibronectin and collagen-IV in the kidney of STZ-diabetic rats. Representative Western immunoblots and the corresponding relative densitometry indicates the basal expressions of TGF-β (A), fibronectin (B), and collagen-IV (C) were significantly elevated in STZ-diabetic rats as compared with control-SD but were reduced by hemin therapy. D, Representative images of kidney sections showing histopathological lesions. Control-SD animals were almost devoid of lesions in the cortex and the medulla except for mild congestions in some sections. However, the STZ-diabetic animals had severe histopathological kidney lesions including glomerulosclerosis, tubular necrosis, intertubular tissue fibrosis, perivascular fibrosis, tubular vacuolization, tubular cast deposition, and tubular and glomerular necrosis. Interestingly, in hemin-treated STZ, these histopathological lesions were greatly attenuated. Magnification, ×200. E, Semiquantitative morphological evaluation showed that hemin reduced renal lesions. Arrows indicate areas of intense lesions. Bars represent means ± SEM (n = 4–6 rats per group). *, $P < .01$ vs STZ; §, $P < .01$ vs control-SD.

dium excretion and enhanced urinary volume observed in hemin-treated STZ may be due to the concomitant enhancement of ANP and its surrogate marker, urinary cGMP (39). Moreover, cGMP is known to enhance natriuresis and diuresis via diuretic-sensitive Na^+ and Cl^- transport in renal-tubular epithelial cells (39). In addition to potentiating ANP, hemin therapy also increased adiponectin levels in plasma and the kidney.

Interestingly, ANP and adiponectin are known to abate fibrosis caused by elevated deposition of the extracellular

matrix (23, 52). Moreover, elevated extracellular matrix/profibrotic proteins such as TGF-β, fibronectin, and collagen would act in conjunction with inflammatory insults triggered by aldosterone via the activation of NF-κB and AP-1 (24) to aggravate glomerular destruction and compromise renal function (53). Similarly, aldosterone stimulates NF-κB that activates cytokines like TNF-α, IL-6, and IL-1β, which in turn stimulate chemokines such as MCP-1 and MIP-1α to promote macrophage infiltration (1, 2, 5, 24, 26) to exacerbate inflammatory insults and damage glomerular tissue causing proteinuria (53) and renal dysfunction in STZ-diabetic rats. However, the synergistic potentiation of the HO-ANP-adiponectin axis by hemin therapy significantly abated NF-κB, TNF-α, IL-6, IL-1β, aldosterone, TGF-β, extracellular matrix deposition, and macrophage infiltration with corresponding reduction of renal lesions and proteinuria, albuminuria but improved creatinine clearance and thus improved renal function. In contrast, the administration of the HO inhibitor, CrMP with hemin or alone abolished the renoprotective effects of hemin, depleted the basal levels of ANP, adiponectin and HO, with robust elevation of NF-κB, TNF-α, IL-6, IL1β, aldosterone, MCP-1, MIP-1α, proteinuria/albuminuria and exacerbated renal impairment, suggesting an important role of the HO-ANP-adiponectin axis in diabetic nephropathy. Moreover, elevated albuminuria is positively correlated to adiponectin deficiency (43). Interestingly, hemin therapy enhanced adiponectin, AMPK, and creatinine clearance concomitantly with parallel reduction of albuminuria and proteinuria. The hemin-dependent enhancement of adiponectin and kidney AMPK may be considered a further confirmation of the intriguing possibility that increasing adiponectin levels or stimulating AMPK may blunt albuminuria/proteinuria and prevent the progression of kidney disease (43, 55).

The concomitant potentiation of ANP and adiponectin by an up-regulated HO system is an important cytoprotective mechanism in renal tissues. Moreover, the activities of HO, ANP, and adiponectin are closely related. Because ANP has been shown to stimulate adiponectin release (56), it is possible that the enhanced production of adiponectin in hemin-treated animals arise from direct stimulation by hemin and/or indirectly via the hemin-dependent potentiation of ANP. Whether these two mechanisms act in concert to synergistically potentiate adiponectin production remains to be clarified in future investigations. On the other hand, ANP enhances the HO system (57, 58), and similarly, the HO system also potentiates ANP (19). The mutual stimulatory effect between ANP and the HO system could synergistically enhance renoprotection given that both ANP and the HO system are cytoprotective (8, 58). The role of ANP in STZ-diabetic animals has been well documented (59). Elevated ANP levels were reportedly accompanied by reduction of renal ANP receptors and a parallel reduction of cGMP levels in isolated glomeruli and inner medullary collecting duct cells in vitro (59). Given that urinary cGMP is a surrogate marker of ANP (41), the depressed levels of urinary cGMP reported in STZ animals in the present study provides more solid evidence of the impaired physiological response of ANP in STZ-diabetes.

Our study also indicates that BP was normotensive in all groups, although STZ-diabetic animals had a modest increase of 5 mm Hg. Because the levels of aldosterone and water retention were increased in STZ-diabetic animals, these observations suggest that increased water retention might be a forerunner to hypertension in STZ-diabetes, so individuals with type 1 diabetes may have increased risk to develop hypertension when they lose the ability to compensate for the early changes (60).

Conclusion

With the high incidence of end-stage renal disease (61), novel therapeutic modalities are needed. Given that end-stage renal disease is common in patients with chronic diseases like diabetes and hypertension (61), two pathophysiological conditions characterized by elevated oxidative/inflammatory insults associated with progressive tissue degradation, severe renal histopathological lesions, and gradual loss of renal function, the potentiation of the HO-ANP-adiponectin axis is important for renoprotection. Moreover, the corresponding reduction of the proinflammatory macrophage M1 phenotype in addition to the abrogation of a variety of different inflammatory agents including MIP-1α, MCP-1, NF-κB, AP-1, TNF-α, IL-6, IL-1β, aldosterone, and extracellular matrix/profibrotic proteins constitutes the multifaceted mechanisms by which hemin therapy reduces proteinuria/albuminuria and improves creatinine clearance, which could be explored in the search for novel therapeutic modalities against renal dysfunction and diabetic nephropathy.

Thus, the formulation of novel therapeutic strategies capable of potentiating the HO-ANP-adiponectin axis could potentially annul a cardinal pathological factor like inflammation that contributes to the progressive development of diabetic nephropathy and would be of great benefit, given the immense burden that diabetes and diabetic nephropathy pose to health care systems.

Acknowledgments

Address all correspondence and requests for reprints to: Dr Joseph Fomusi Ndisang, Department of Physiology, Uni-

versity of Saskatchewan College of Medicine, 107 Wiggins Road, Saskatoon, Saskatchewan, Canada S7N 5E5. E-mail: joseph.ndisang@usask.ca.

This work was supported by a grant from the Heart and Stroke Foundation of Saskatchewan, Canada (to J.F.N.).

Disclosure Summary: The authors have nothing to disclose.

References

1. **Navarro-Gonzalez JF, Mora-Fernandez C, Muros de Fuentes M, Garcia-Perez J.** Inflammatory molecules and pathways in the pathogenesis of diabetic nephropathy. *Nat Rev Nephrol*. 2011;7:327–340.
2. **Navarro-Gonzalez JF, Mora-Fernandez C.** Inflammatory pathways. *Contrib Nephrol*. 2011;170:113–123.
3. **Strawn WB.** [Pathophysiological and clinical implications of AT(1) and AT(2) angiotensin II receptors in metabolic disorders: hypercholesterolaemia and diabetes]. *Drugs 62 Spec No*. 2002;1:31–41.
4. **Iwamoto M, Mizuiri S, Arita M, Hemmi H.** Nuclear factor-κB activation in diabetic rat kidney: evidence for involvement of P-selectin in diabetic nephropathy. *Tohoku J Exp Med*. 2005;206:163–171.
5. **Cifuentes M, Fuentes C, Tobar N, et al.** Calcium sensing receptor activation elevates proinflammatory factor expression in human adipose cells and adipose tissue. *Mol Cell Endocrinol*. 2012;361:24–30.
6. **Ndisang JF.** Role of heme oxygenase in inflammation, insulin-signalling, diabetes and obesity. *Mediators Inflamm*. 2010;2010:359732.
7. **Gordon S, Martinez FO.** Alternative activation of macrophages: mechanism and functions. *Immunity*. 2010;32:593–604.
8. **Jadhav A, Torlakovic E, Ndisang JF.** Hemin therapy attenuates kidney injury in deoxycorticosterone acetate-salt hypertensive rats. *Am J Physiol Renal Physiol*. 2009;296:F521–F534.
9. **Mezzano S, Aros C, Droguett A, et al.** NF-κB activation and overexpression of regulated genes in human diabetic nephropathy. *Nephrol Dial Transplant*. 2004;19:2505–2512.
10. **Tiwari S, Ndisang JF.** The heme oxygenase system and type 1 diabetes. *Curr Pharm Des*. [published online July 25, 2013].
11. **Tiwari S, Ndisang JF.** Heme oxygenase system and hypertension: a comprehensive insight. *Curr Pharm Des*. [published online July 25, 2013].
12. **Mishra M, Ndisang JF.** A critical and comprehensive insight on heme oxygenase and related products including carbon monoxide, bilirubin, biliverdin and ferritin in type-1 and type-2 diabetes. *Curr Pharm Des*. [published online July 25, 2013].
13. **Jadhav A, Ndisang JF.** Treatment with heme arginate alleviates adipose tissue inflammation and improves insulin sensitivity and glucose metabolism in a rat model of human primary aldosteronism. *Free Radic Biol Med*. 2012;53:2277–2286.
14. **Ndisang JF, Jadhav A.** Up-regulating the hemeoxygenase system enhances insulin sensitivity and improves glucose metabolism in insulin-resistant diabetes in Goto-Kakizaki rats. *Endocrinology*. 2009;150:2627–2636.
15. **Ndisang JF, Jadhav A.** Heme oxygenase system enhances insulin sensitivity and glucose metabolism in streptozotocin-induced diabetes. *Am J Physiol Endocrinol Metab*. 2009;296:E829–E841.
16. **Ndisang JF, Jadhav A.** The heme oxygenase system attenuates pancreatic lesions and improves insulin sensitivity and glucose metabolism in deoxycorticosterone acetate hypertension. *Am J Physiol Regul Integr Comp Physiol*. 2010;298:R211–R223.
17. **Ndisang JF, Lane N, Jadhav A.** Upregulation of the heme oxygenase system ameliorates postprandial and fasting hyperglycemia in type 2 diabetes. *Am J Physiol Endocrinol Metab*. 2009;296:E1029–E1041.
18. **Ndisang JF, Lane N, Syed N, Jadhav A.** Up-regulating the heme oxygenase system with hemin improves insulin sensitivity and glucose metabolism in adult spontaneously hypertensive rats. *Endocrinology*. 2010;151:549–560.
19. **Ndisang JF, Jadhav A.** Heme arginate therapy enhanced adiponectin and atrial natriuretic peptide, but abated endothelin-1 with attenuation of kidney histopathological lesions in mineralocorticoid-induced hypertension. *J Pharmacol Exp Ther*. 2010;334:87–98.
20. **Ndisang JF.** The heme oxygenase system selectively modulates proteins implicated in metabolism, oxidative stress and inflammation in spontaneously hypertensive rats. *Curr Pharm Des*. [published online July 25, 2013].
21. **Moro C, Klimcakova E, Lolmede K, et al.** Atrial natriuretic peptide inhibits the production of adipokines and cytokines linked to inflammation and insulin resistance in human subcutaneous adipose tissue. *Diabetologia*. 2007;50:1038–1047.
22. **Folco EJ, Rocha VZ, Lopez-Ilasaca M, Libby P.** Adiponectin Inhibits pro-inflammatory signaling in human macrophages independent of interleukin-10. *J Biol Chem*. 2009;284:25569–25575.
23. **Piechota M, Banach M, Irzmanski R, et al.** N-terminal brain natriuretic propeptide levels correlate with procalcitonin and C-reactive protein levels in septic patients. *Cell Mol Biol Lett*. 2007;12:162–175.
24. **Li X, Meng Y, Wu P, Zhang Z, Yang X.** Angiotensin II and aldosterone stimulating NF-κB and AP-1 activation in hepatic fibrosis of rat. *Regul Pept*. 2007;138:15–25.
25. **Ding W, Yang L, Zhang M, Gu Y.** Chronic inhibition of nuclear factor κ B attenuates aldosterone/salt-induced renal injury. *Life Sci*. 2012;90:600–606.
26. **Wu YP, Proia RL.** Deletion of macrophage-inflammatory protein 1α retards neurodegeneration in Sandhoff disease mice. *Proc Natl Acad Sci USA*. 2004;101:8425–8430.
27. **Ndisang JF, Lane N, Jadhav A.** The heme oxygenase system abates hyperglycemia in Zucker diabetic fatty rats by potentiating insulin-sensitizing pathways. *Endocrinology*. 2009;150:2098–2108.
28. **Jadhav A, Torlakovic E, Ndisang JF.** Interaction among heme oxygenase, nuclear factor-κB, and transcription activating factors in cardiac hypertrophy in hypertension. *Hypertension*. 2008;52:910–917.
29. **Ndisang JF, Lane N, Jadhav A.** Crosstalk between the heme oxygenase system, aldosterone, and phospholipase C in hypertension. *J Hypertens*. 2008;26:1188–1199.
30. **Ndisang JF, Jadhav A.** Hemin therapy suppresses inflammation and retroperitoneal adipocyte hypertrophy to improve glucose metabolism in obese rats co-morbid with insulin resistant type 2 diabetes. *Diabetes Obes Metab*. 2013;15(11):1029–1039.
31. **Ndisang JF, Mishra M.** The heme oxygenase system selectively suppresses the proinflammatory macrophage m1 phenotype and potentiates insulin signaling in spontaneously hypertensive rats. *Am J Hypertens*. 2013;26:1123–1131.
32. **Turkseven S, Kruger A, Mingone CJ, et al.** Antioxidant mechanism of heme oxygenase-1 involves an increase in superoxide dismutase and catalase in experimental diabetes. *Am J Physiol Heart Circ Physiol*. 2005;289:H701–H707.
33. **Vreman HJ, Ekstrand BC, Stevenson DK.** Selection of metalloporphyrin heme oxygenase inhibitors based on potency and photoreactivity. *Pediatr Res*. 1993;33:195–200.
34. **Jadhav A, Ndisang JF.** Heme arginate suppresses cardiac lesions and hypertrophy in deoxycorticosterone acetate-salt hypertension. *Exp Biol Med (Maywood)*. 2009;234:764–778.
35. **Jadhav A, Tiwari S, Lee P, Ndisang JF.** The heme oxygenase system selectively enhances the anti-inflammatory macrophage-m2 phenotype, reduces pericardial adiposity, and ameliorated cardiac injury in diabetic cardiomyopathy in Zucker diabetic fatty rats. *J Pharmacol Exp Ther*. 2013;345:239–249.
36. **Matavelli LC, Siragy HM.** Reduction of aldosterone production

improves renal oxidative stress and fibrosis in diabetic rats. *J Cardiovasc Pharmacol*. 2013;61(1):17–22.
37. **Shoham S, Bejar C, Kovalev E, Weinstock M.** Intracerebroventricular injection of streptozotocin causes neurotoxicity to myelin that contributes to spatial memory deficits in rats. *Exp Neurol*. 2003; 184:1043–1052.
38. **Chen NY, Chen WY, Bellush L, et al.** Effects of streptozotocin treatment in growth hormone (GH) and GH antagonist transgenic mice. *Endocrinology*. 1995;136:660–667.
39. **Pandey KN.** Biology of natriuretic peptides and their receptors. *Peptides*. 2005;26:901–932.
40. **Ndisang JF, Jadhav A.** Heme-arginate suppresses phospholipase C and oxidative stress in the mesenteric arterioles of mineralcorticoid-induced hypertensive rats. *Hypertens Res*. 2010;33:338–347.
41. **Benigni A, Zoja C, Zatelli C, et al.** Vasopeptidase inhibitor restores the balance of vasoactive hormones in progressive nephropathy. *Kidney Int*. 2004;66:1959–1965.
42. **Burgess A, Li M, Vanella L, et al.** Adipocyte heme oxygenase-1 induction attenuates metabolic syndrome in both male and female obese mice. *Hypertension*. 2010;56:1124–1130.
43. **Sharma K, Ramachandrarao S, Qiu G, et al.** Adiponectin regulates albuminuria and podocyte function in mice. *J Clin Invest*. 2008; 118:1645–1656.
44. **Yamauchi T, Kamon J, Minokoshi Y, et al.** Adiponectin stimulates glucose utilization and fatty-acid oxidation by activating AMP-activated protein kinase. *Nat Med*. 2002;8:1288–1295.
45. **DiPetrillo K, Coutermarsh B, Soucy N, Hwa J, Gesek F.** Tumor necrosis factor induces sodium retention in diabetic rats through sequential effects on distal tubule cells. *Kidney Int*. 2004;65:1676–1683.
46. **Yang J, Pollock JS, Carmines PK.** NADPH oxidase and PKC contribute to increased Na transport by the thick ascending limb during type 1 diabetes. *Hypertension*. 2012;59:431–436.
47. **Lawrence T, Natoli G.** Transcriptional regulation of macrophage polarization: enabling diversity with identity. *Nat Rev Immunol*. 2011;11:750–761.
48. **Gordon S.** Alternative activation of macrophages. *Nat Rev Immunol*. 2003;3:23–35.
49. **Aki K, Shimizu A, Masuda Y, et al.** ANG II receptor blockade enhances anti-inflammatory macrophages in anti-glomerular basement membrane glomerulonephritis. *Am J Physiol Renal Physiol*. 2010;298:F870–F882.
50. **Satoh-Asahara N, Shimatsu A, Sasaki Y, et al.** Highly purified eicosapentaenoic acid increases interleukin-10 levels of peripheral blood monocytes in obese patients with dyslipidemia. *Diabetes Care*. 2012;35:2631–2639.
51. **Chatterjee PK, Hawksworth GM, McLay JS.** Cytokine-stimulated nitric oxide production in the human renal proximal tubule and its modulation by natriuretic peptides: a novel immunomodulatory mechanism? *Exp Nephrol*. 1999;7:438–448.
52. **Bertolani C, Marra F.** Role of adipocytokines in hepatic fibrosis. *Curr Pharm Des*. 2010;16:1929–1940.
53. **Finer G, Schnaper HW, Kanwar YS, Liang X, Lin HY, Hayashida T.** Divergent roles of Smad3 and PI3-kinase in murine adriamycin nephropathy indicate distinct mechanisms of proteinuria and fibrogenesis. *Kidney Int*. 2012;82:525–536.
54. **Tiwari S, Ndisang JF.** The role of obesity in cardiomyopathy and nephropathy. *Curr Pharm Des*. [published online July 25, 2013].
55. **Lee MJ, Feliers D, Mariappan MM, et al.** A role for AMP-activated protein kinase in diabetes-induced renal hypertrophy. *Am J Physiol Renal Physiol*. 2007;292:F617–F627.
56. **Birkenfeld AL, Boschmann M, Engeli S, et al.** Atrial natriuretic peptide and adiponectin interactions in man. *PLoS One*. 2012;7: e43238.
57. **Kiemer AK, Bildner N, Weber NC, Vollmar AM.** Characterization of heme oxygenase 1 (heat shock protein 32) induction by atrial natriuretic peptide in human endothelial cells. *Endocrinology*. 2003;144:802–812.
58. **Polte T, Hemmerle A, Berndt G, Grosser N, Abate A, Schroder H.** Atrial natriuretic peptide reduces cyclosporin toxicity in renal cells: role of cGMP and heme oxygenase-1. *Free Radic Biol Med*. 2002; 32:56–63.
59. **Sechi LA, Valentin JP, Griffin CA, et al.** Receptors for atrial natriuretic peptide are decreased in the kidney of rats with streptozotocin-induced diabetes mellitus. *J Clin Invest*. 1995;95:2451–2457.
60. **Patel KP.** Volume reflex in diabetes. *Cardiovasc Res*. 1997;34: 81–90.
61. **Rosamond W, Flegal K, Furie K, et al.** Heart disease and stroke statistics-2008 update: a report from the American Heart Association Statistics Committee and Stroke Statistics Subcommittee. *Circulation*. 2008;117:e25–e146.